

## A ROTOR POSITION ERROR COMPENSATION STRATEGY FOR PERMANENT MAGNET SYNCHRONOUS MOTOR BASED ON PHASE-LOCKED LOOP

Zhouji LI <sup>1,\*</sup>, Intan Irieyana Bint ZULKEPLI <sup>2</sup>

*The control methods of permanent magnet synchronous motors (PMSM) rely on rotor position information. However, the rotor position information obtained by the flux observer consists of estimation errors caused by non-ideal factors such as loop filters and motor parameter deviations. In this paper, we first analyze the causes of the phase estimation errors, then use the phase-locked loop (PLL) to reconstruct and compensate for the rotor position error to improve the observer's observation accuracy. The position error compensation strategy is robust to phase delay and independent of motor parameters. Simulation results verify that the method can effectively reduce the observation error and improve the accuracy estimation of rotor position and speed to achieve a better sensorless control effect of a PMSM.*

**Keywords:** PMSM, position error compensation strategy, PLL

### Nomenclature

$u_\alpha, u_\beta$	Rotor phase voltages in stationary reference
$i_\alpha, i_\beta$	Rotor phase currents in stationary reference
$L_\alpha, L_\beta$	Phase inductance in stationary reference
$L_d, L_q$	Phase inductance in rotational reference
$e_\alpha, e_\beta$	Back EMF in rotational reference
$\omega_e$	Electrical angular velocity
R	Stator winding resistance

<sup>1\*</sup> Ph.D. candidate, Faculty of Engineering & Built Environment, Lincoln University College, Malaysia, \* Corresponding author: e-mail: zhouji@lincoln.edu.my

<sup>2</sup> Professor, Faculty of Engineering & Built Environment, Lincoln University College, Malaysia, e-mail: irieyanaintan@lincoln.edu.my

---

$\theta_e$	Actual rotor position
$\hat{\theta}_e$	Estimated rotor position
$\psi_f$	Actual flux linkage
$\hat{\psi}_f$	Estimated flux linkage
$\omega_L$	Cut-off frequency of HPF
$\omega_H$	Cut-off frequency of LPF

## 1. Introduction

Permanent magnet synchronous motor (PMSM) is characterized by high power density, a compact footprint, and lightweight construction, making it a prevalent choice in electric vehicles [1]. PMSM control relies on precise rotor position information, which can be obtained from position sensors. However, this mechanical control scheme increases the volume of the motor controller and the production costs. Conversely, it reduces the post-maintainability and reliability of the control system. For these reasons, the sensorless motor control scheme has become a subject of considerable research interest as a potential control method for PMSM.

The sensorless control methods of PMSM can be divided into two categories: single-injecting and based-model methods. Single-injecting methods are based on the motor's saliency effect, necessitating an additional band-pass filter. These methods are effective at low and medium speeds; however, as the speed increases, the frequencies between the high-frequency injected current and the fundamental frequency current approach result in a decrease in filter resolution and a concomitant reduction in estimation effectiveness. Furthermore, these methods do not apply to surface-mounted permanent magnet synchronous motors (SPMSMs), which exhibit low saliency effects [2]. The model-based methods estimate the rotor position from the state observer based on back electromotive force. This method includes the model reference adaptive system [3-4], the extended Kalman filter [5], the sliding mode observer [6-7], the flux observer [8], and so forth.

The Flux Observer employs a voltage equation for the motor to calculate the component of the rotor flux linkage in the  $\alpha$ - $\beta$  coordinate axis, thereby estimating the rotor position. This method offers simplicity and a fast-dynamic response, contributing to its increased usage. However, the voltage equation model contains a pure integral, susceptible to issues such as DC bias and integral drift. The

sensorless control algorithm is also vulnerable to non-ideal factors that can cause significant rotor position estimation errors.

To eliminate the 6k signal pulsation caused by the nonlinearity of the inverter and the space harmonics, literature [9] proposes a position estimation method based on an adaptive filter. Literature [10-11] enhances the precision of position estimation by online identifying motor parameters. However, the complexity of the motor parameter identifying model reduces the system's real-time performance. To eliminate the effect of harmonics, Literature [12] proposes the use of a synchronized frequency extraction filter, which can directly extract the fundamental component of the signal. In literature [13], a closed-loop position error compensation method is proposed based on the error characteristic quantity and the characteristic component of the rotor position error on the straight axis for closed-loop adjustment of the rotor position. This method is relatively straightforward to implement, although the inductor influences it. Literature [14] proposes a dual phase-locked loop based on quadrature phase-locked loops, which enables the reconstruction of signal delay and thus compensates for position errors. Gu et al. proposed a novel EMF-SMO based on a double phase-locked loop, in which the delayed reconstructed current signal is introduced using a non-ideal factor. The double phase-locked loop refers to a system in which the reconstructed current signal and the estimated position signal are phase-locked twice, thus enabling the phase estimation error to be fully compensated without the need for quantitative calculation. In the literature [16], the position error compensation was achieved by tracking the minimum current. This method is notable for its robustness, as it is independent of any parameters. However, it is susceptible to current jitter in the steady state, which can affect the system's stability.

Chapter 2 provided an overview of the fundamental principles of the flux linkage observer and examined the impact of non-ideal factors on the estimation of rotor position error. Chapter 3 presents a novel PLL error compensation strategy founded upon the PLL's fundamental principles. The accuracy of the estimated position signal has been improved by implementing a comprehensive solution that addresses the estimation error of loop delay. Chapter 4 presents a simulation of the novel PLL error compensation strategy using SPMSM to verify its effectiveness.

## 2. Rotor Flux Observer for PMSM

### 2.1 Position Observer Construction

The model of PMSM in stationary reference is usually described as follows:

$$\begin{bmatrix} u_\alpha \\ u_\beta \end{bmatrix} = \begin{bmatrix} R + \frac{d}{dt}L_\alpha & \frac{d}{dt}L_{\alpha\beta} \\ \frac{d}{dt}L_{\alpha\beta} & R + \frac{d}{dt}L_\beta \end{bmatrix} \begin{bmatrix} i_\alpha \\ i_\beta \end{bmatrix} + \omega_e \psi_f \begin{bmatrix} -\sin\theta_e \\ \cos\theta_e \end{bmatrix} \quad (1)$$

For the phase inductance, whose values are:

$$\begin{cases} L_\alpha = L_0 + L_1 \cos 2\theta_e \\ L_\beta = L_0 - L_1 \cos 2\theta_e \\ L_{\alpha\beta} = L_1 \sin 2\theta_e \\ L_0 = (L_d + L_q)/2 \\ L_1 = (L_d - L_q)/2 \end{cases}$$

For SPMSM,  $L_d = L_q$ , to simplify equation (1), the mathematical model can be written as follows:

$$\begin{bmatrix} u_\alpha \\ u_\beta \end{bmatrix} = \begin{bmatrix} R + \frac{d}{dt} L_q & 0 \\ 0 & R + \frac{d}{dt} L_q \end{bmatrix} \begin{bmatrix} i_\alpha \\ i_\beta \end{bmatrix} + \omega_e \psi_f \begin{bmatrix} -\sin \theta_e \\ \cos \theta_e \end{bmatrix} \quad (2)$$

The back EMF for each phase can be described as follows:

$$\begin{bmatrix} e_\alpha \\ e_\beta \end{bmatrix} = \omega_e \psi_f \begin{bmatrix} -\sin \theta_e \\ \cos \theta_e \end{bmatrix} \quad (3)$$

The flux linkage is defined as an integral of the back EMF. According to equations (2) and (3), the flux linkage of the rotor can be calculated as follows:

$$\begin{bmatrix} \psi_{r,\alpha} \\ \psi_{r,\beta} \end{bmatrix} = \int \left( \begin{bmatrix} u_\alpha \\ u_\beta \end{bmatrix} - \begin{bmatrix} R + \frac{d}{dt} L_\alpha & 0 \\ 0 & R + \frac{d}{dt} L_\alpha \end{bmatrix} \begin{bmatrix} i_\alpha \\ i_\beta \end{bmatrix} \right) dt \quad (4)$$

The flux observer is the application of equation (4) for the estimation of the rotor flux linkage in the  $\alpha$ -axis and  $\beta$ -axis. Subsequently, the estimated rotor position can be obtained through the application of an arctangent operation, as detailed below:

$$\hat{\theta}_r = \arctan \frac{\hat{\psi}_{r,\alpha}}{\hat{\psi}_{r,\beta}} \quad (5)$$

Therefore, the rotor speed can be obtained as follows:

$$\omega_e = \frac{d\theta_r}{dt} \quad (6)$$

## 2.2 Position Estimated Error Analysis

In practical applications, conventional flux observers have been observed to produce fundamental frequency bias, motor parameter bias, and current sampling bias. These arise due to the sampling accuracy, measurement noise, filters, and other factors. The presence of these biases has been demonstrated to reduce the accuracy of the observations produced.

### 2.2.1 Fundamental Frequency Bias

A pure integrator is vulnerable to the DC offset and the initial value of the integral. In consideration of the input to the pure integrator, which is a sinusoidal function with a small DC offset, the resulting output is as follows:

$$\int_{t_0}^t (\omega A \sin \omega t + B) dt = -A \cos \omega t + Bt + C_0 \quad (7)$$

As the time increases, the DC offset  $Bt$  increases until it reaches saturation, and the initial value of the integral  $C_0$  produces the offset. This is the reason why it is difficult to estimate with high accuracy. A high-pass filter (HPF) can be used in a series of flux observers with a pure integrator to reduce the DC offset. Additionally, a low-pass filter (LPF) is connected in series with the objective of eliminating high-frequency harmonics and interference signals. The structure diagram of the rotor flux observer is shown in Fig. 1.

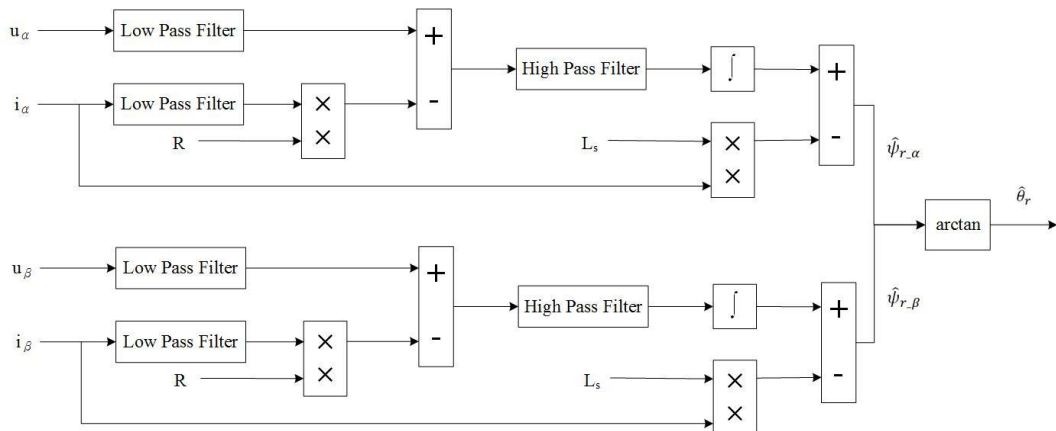


Fig.1. The structure diagram of the rotor flux observer

Nevertheless, the application of HPF and LPF results in the emergence of a fundamental frequency bias  $\Delta\theta_f$ , which can be expressed as follows:

$$\Delta\theta_f = \frac{\pi}{2} - \arctan \frac{\omega_e}{\omega_H} - \arctan \frac{\omega_e}{\omega_L} \quad (8)$$

From equation (8), the position error caused by loop filters is quantifiable and increases as the fundamental frequency rises.

### 2.2.2 Motor Parameter Bias

The motor parameter encompasses a range of factors, including inductance bias, resistance bias, voltage sampling bias, and current sampling bias, among others. It is challenging to quantify and compensate for these types of errors. To

illustrate,  $L_s$  is highly susceptible to saturation effects. Identify inductance bias  $\Delta L_s = L_s - \hat{L}_s$ ,  $\hat{L}_s$  is estimated inductance. If using  $i_d = 0$  control model, stator current look-ahead rotor flux is  $\pi/2$ , the position error resulting from the inductance bias can be calculated as follows:

$$\Delta\theta_L = \arctan \frac{\Delta L_s |i_s|}{|\psi_r|} \quad (9)$$

Due to the existence of the cumulative amount of parameter bias, if pure integration is used directly, the integration result will drift or even saturate. Thus affecting the flux linkage calculation result and leading to the inability to obtain the correct rotor position information.

### 2.2.3 Sampling Time Delay Bias

The analog signal sampling process typically incorporates a zero-order hold (ZOH), which introduces the loop time delay. If the sampling period is represented by  $T_s$ , the time delay is  $T_s/2$  and is a constant time delay. The impact of the constant time delay on phase estimation error is exacerbated as the rotational speed increases.

In conclusion, the rotor flux observer introduces a degree of positional inaccuracy in the estimation of rotor position. The resulting position error can be expressed as follows:

$$\Delta\theta_{total} = \sum_{i=1,2,\dots,m}^m (\Delta\theta_f) + f\Delta(L_s, R_s, \dots) + \frac{T_s}{2} \quad (10)$$

## 3. A Novel Rotor Position Error Compensation Strategy

### 3.1 PLL Error Compensation Strategy

In PMSM, the actual rotor position  $\theta_r$  is maintained at a fixed phase relative to the stator magnetic chain  $\psi_s$ . In the “id=0” control mode, the current integral  $\int i_s dt$  maintains a constant phase relationship with  $\psi_s$ . Hypothesis: the estimated stator flux linkage  $\hat{\psi}_s = \int i_s dt$  is  $\Delta\theta$  phase behind the actual stator flux linkage  $\psi_s$ . It utilizes current integral and filter to reconstruct the current delay signal  $\int i_{s\_d} dt$ , which maintains the phase  $\Delta\theta$  relationship with  $\int i_s dt$ .

A phase-locked loop (PLL) employs a feedback mechanism to compare the frequency and phase of an input signal with a reference signal and adjusts as necessary to ensure that the frequency and phase of the input signal remain in phase with the reference signal. We use phase-locked to lock  $\int i_{s\_d} dt$  and  $\hat{\psi}_s$ , when  $\int i_{s\_d} dt$  maintains a consistent phase alignment with  $\hat{\psi}_s$ ,  $\int i_s dt$  are also locked with  $\psi_s$  at same phase. At this point, the phase-locked loop generates a

compensation angle  $\Delta\theta$ , which compensates for the position estimation error. Fig. 2 shows the fundamental principle of the position compensation.

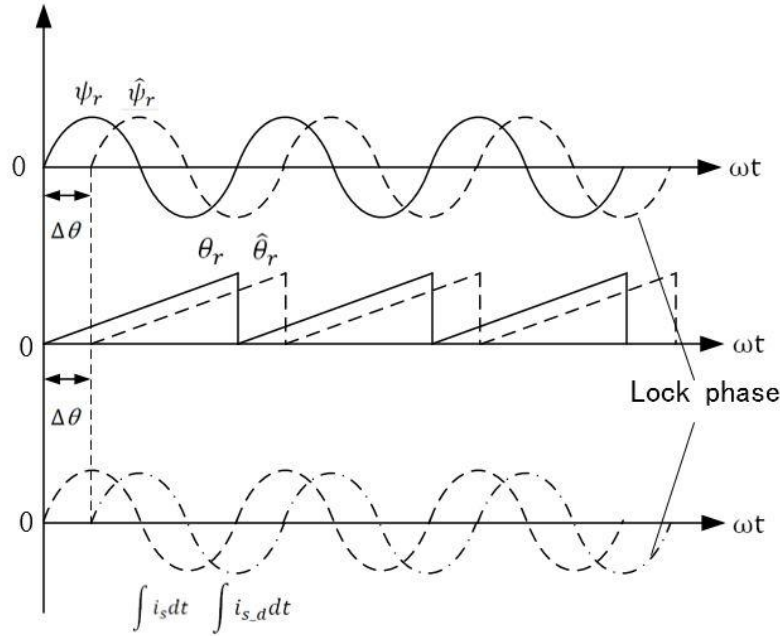


Fig.2. The principle of the position error compensation by lock phase

A phase-locked loop error compensation strategy based on the appeal principle is proposed. Following the application of a low-pass filter and a high-pass filter, the input signals  $i_\alpha$  and  $i_\beta$  are integrated to yield  $\int i_{\alpha,d} dt$  and  $\int i_{\beta,d} dt$ , and then phase lock with  $\hat{\psi}_\alpha$  and  $\hat{\psi}_\beta$ . Once they are aligned in phase, the PLL generates the compensation angle  $\Delta\theta$ , the value of which is then applied to the estimated angle  $\hat{\theta}_r$ . Ultimately, this process compensates the rotor position error, thereby obtaining the accurate rotor position  $\hat{\theta}_{r,c}$ . Fig. 3 presents a block diagram of the PLL position error compensation.

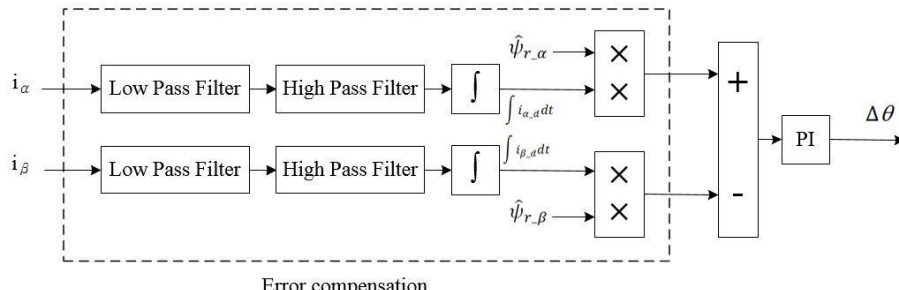


Fig.3. The block diagram of PLL position error compensation

### 3.2 Sensorless Control Scheme Based on Rotor Flux Observer with PLL Error Compensation Strategy

In order to enhance the precision of the sensorless field-oriented control (FOC) system of PMSM and to optimize the performance of the drive system, it would be beneficial to integrate the previously proposed PLL error compensation strategy into the conventional flux observer, thereby achieving a comprehensive correction of the position signal estimation error. Fig. 4 illustrates the block diagram of a sensorless FOC system based on a flux observer with PLL error compensation. The sampling currents and voltages are fed into a novel flux observer with PLL position error compensation in order to obtain the estimated rotor position information. Subsequently, the motor speed information is obtained through a speed estimator, which is then fed back into the speed loop and current loop of the motor control system.

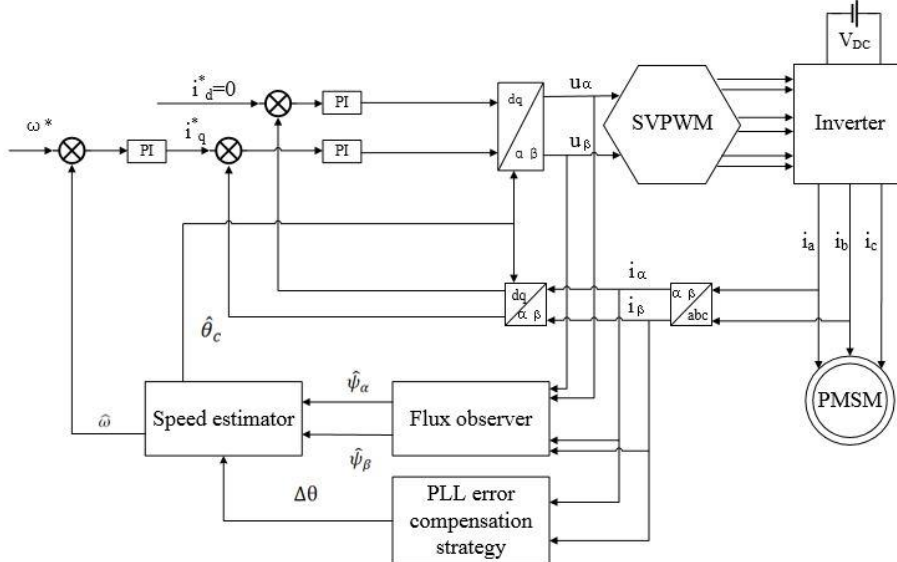


Fig.4. Block diagram of sensorless control FOC system based on the flux observer with PLL error compensation

The PLL error compensation strategy proposed in this paper considers the impact of rotor position estimated error resulting from various non-ideal factors and aims to achieve comprehensive without explicitly quantifying the estimated error. In contrast, this strategy does not introduce any sensitive parameters, which could reduce the operational stability of the system.

## 4. Simulation Results and Analysis

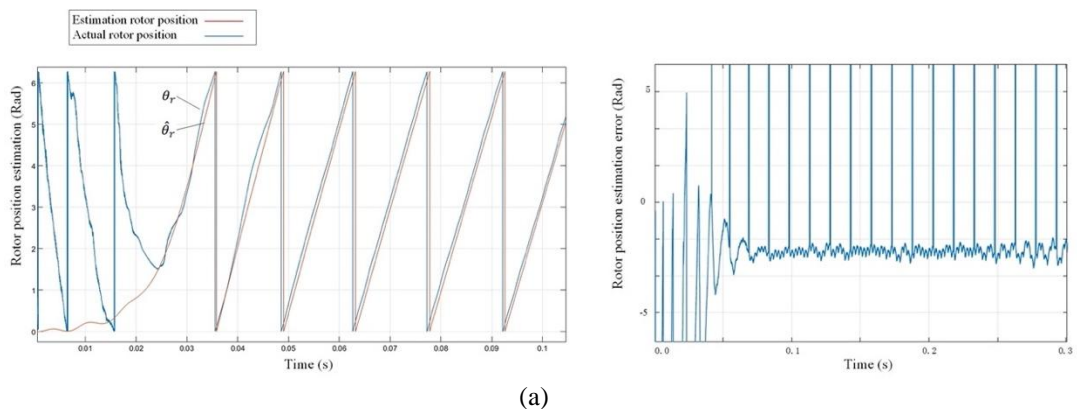
In order to ascertain the efficacy of the PLL error compensation strategy proposed, a comprehensive simulation of SPMSM is conducted. The motor

parameters are presented in tabular form in Table 1. As illustrated in Fig. 4, a simulation model of an SPMSM sensorless drive based on a field-oriented control (FOC) strategy and  $id=0$  control has been constructed within the Simulink programming environment.

Table 1 Parameters of SPMSM

Quantity	Value	Unit
Number of pole pairs	4	
Stator phase resistance	0.958	$\Omega$
Stator inductance	5.25	mH
Flux linkage	0.958	Wb
Direct voltage	311	V
Coefficient of friction	0.003	$\text{Kg} \cdot \text{m}^2$
Rated speed	1000	rpm
Switch frequency	10	kHz
Sampling time	10	$\mu\text{s}$

Fig. 5 shows the simulation results of the estimated rotor position  $\hat{\theta}_r$  and the actual rotor position  $\theta_r$  of the SPMSM by the different kinds of flux observers at rated speed 1000 rpm. Fig. 5(a) illustrates that the conventional flux observer yields an estimation rotor position error of approximately 2.2 rad, whereas Fig. 5(b) demonstrates that the PLL error compensation strategy results in an estimation rotor position error of nearly 0 rad. In conventional flux observer without the compensation strategy, the phase of the current integral  $\int i_{s\_delay} dt$  behind the estimation rotor flux  $\hat{\psi}_r$  as shown in Fig. 6(a), however, the phase between the  $\hat{\psi}_r$  and  $\int i_{s\_delay} dt$  is aligned when the PLL error compensation strategy is employed, as illustrated in Fig. 6(b). The simulation results substantiate the efficacy and superiority of the proposed strategy.



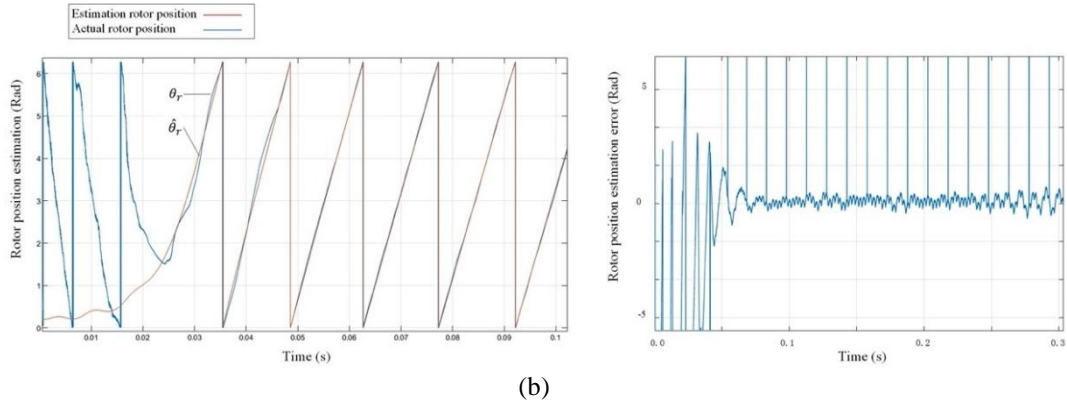


Fig. 5. Simulation results of rotor position estimation using different observers. (a) Conventional flux observer, (b) Flux observer with PLL error compensation strategy

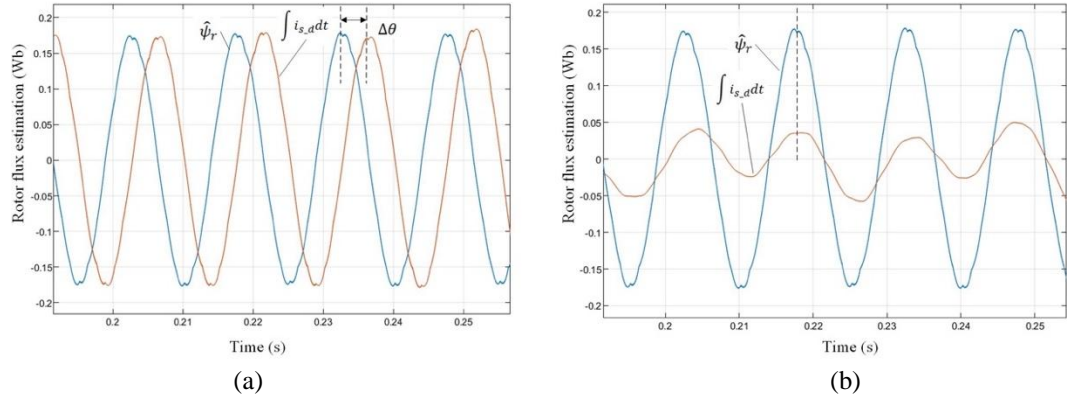


Fig.6. Simulation results of the phase between the rotor flux estimation and the current. (a) Based on the conventional flux observer without the compensation strategy, (b) Based on the PLL error compensation strategy

Experiments were conducted to analysis the influence of varying estimated angular error when stator inductance ( $L$ ) was modified to verify further the effect of motor parameter variations on the system's stability. Fig. 7 shows the simulation results of the rotor position estimation on  $L_s = 5.25 \text{ mH}$  and  $L_s = 525 \text{ mH}$ . It can be observed that the estimation rotor position error increases with the addition of stator inductance. When  $L_s = 525 \text{ mH}$ , the PLL error compensation strategy remains operational.

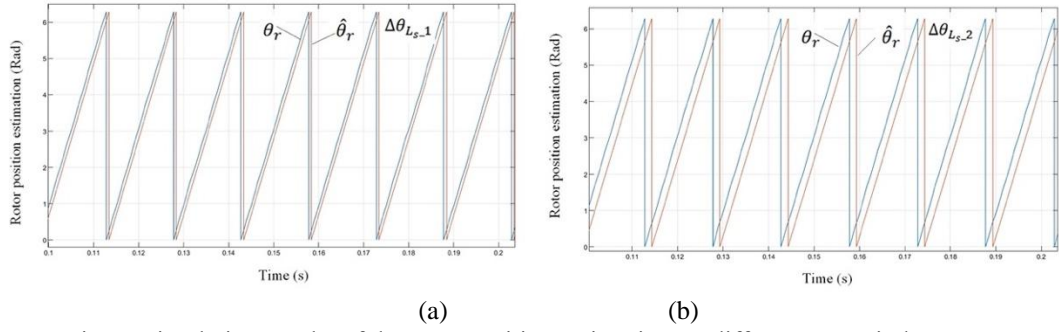


Fig. 7. Simulation results of the rotor position estimation on different stator inductance.  
(a)  $L_s=5.25\text{mH}$ , (b)  $L_s=525\text{mH}$

## 5. Conclusion

This paper proposes a novel position error compensation strategy for the rotor flux observer based on the sensorless control system for SPMSM. The strategy provides compensation for errors resulting from non-ideal factors introduced by loop filters and inductor parameter bias. The operational principle is to obtain the rotor position error by estimating the flux linkage through the flux observer and then phase-lock the estimated position signal with the current integral signal using PLL, which enables the full compensation of the phase estimation error. The proposed method offers the benefit of full compensation for position estimation error without the necessity for precise quantification. The simulation results demonstrate that the proposed rotor position error compensation strategy is effective and robust to sensitive parameters such as  $L_s$ . Consequently, the motor is able to achieve a higher degree of accuracy in rotor position estimation through position error compensation.

## R E F E R E N C E S

- [1] *Gerada D, Mebarki A, Brown N L, et al.* “High-speed electrical machines: Technologies, trends, and developments”. *IEEE transactions on industrial electronics*, **vol. 61**, no. 6, Sep. 2013, pp. 2946-2959.
- [2] *J.M. Liu, & Z. Q. Zhu*, “Novel sensorless control strategy with injection of high-frequency pulsating carrier signal into stationary reference frame”. *IEEE Transactions on Industry Applications*, **vol. 50**, no. 4, Jul. 2013, pp. 2574-2583
- [3] *R. Kumar, S. Das, P. Syam, & A. K. Chattopadhyay*, “Review on model reference adaptive system for sensorless vector control of induction motor drives”. *IET Electric Power Applications*, **vol. 9**, no. 7, Aug. 2015, pp. 496-511.
- [4] *H.S Zhang, P. Wang, & B.C. Han*, “Rotor position detection of high-speed permanent magnet synchronous motor based on fuzzy PI model reference adaptation”. *Chinese Journal of Electrical Engineering*, **vol. 34**, no. 12, May 2014, pp. 1889-1896.
- [5] *T. Shi, Z. Wang, & C Xia*, “Speed measurement error suppression for PMSM control system using self-adaption Kalman observer”. *IEEE Transactions on Industrial Electronics*, **vol. 62**, no. 5, May 2014, pp. 2753-2763.

- [6] *R. Sreejith, & B. Singh*, “Sensorless predictive control of SPMSM-driven light EV drive using modified speed adaptive super twisting sliding mode observer with MAF-PLL. IEEE Journal of Emerging and Selected Topics in Industrial Electronics”, **vol. 2**, no. 1, Jan. 2020, pp. 42-52.
- [7] *R. Sreejith, & B. Singh*, “Sensorless predictive current control of PMSM EV drive using DSOGI-FLL based sliding mode observer”. IEEE Transactions on Industrial Electronics, **vol. 68**, no. 7, Jul. 2020, pp. 5537-5547.
- [8] *S.Y. Wang, Z.P. Luo, S.Q. Zhang, Y. Han, & S.S. Wang*, “Optimized feedback compensated closed-loop stator chain observer”. Micromotor, **vol. 55**, no. 8, Aug. 2022, (008), pp.80-94.
- [9] *H. Wang, W.L. Pan, & X. Wu*, “An adaptive filtering method for rotor position estimation of permanent magnet synchronous motor”. Journal of Electrical Machines and Control, **vol. 23**, no. 11, Nov. 2019, pp. 1-9.
- [10] *X. C. Li, P. Y. L. Y. Zhang, & S. K. Ma*, “Position sensorless control of permanent magnet synchronous motor with parameter identification”. Journal of Electrotechnology, **vol. 31**, no. 14, Aug. 2016, pp. 139-147.
- [11] *X. Song, J. Fang, B. Han, & S. Zheng*, “Adaptive compensation method for high-speed surface PMSM sensorless drives of EMF-based position estimation error”. IEEE Transactions on Power Electronics, **vol. 31**, no. 2, Feb. 2016, pp. 1438-1449.
- [12] *H. Nian, J.W. Li, & Z.Q. Wan*, “Position sensorless control of permanent magnet wind turbine based on online parameter identification”. Chinese Journal of Electrical Engineering, **vol. 32**, no. 12, Dec. 2012, pp. 146-154.
- [13] *K. Y. Huang, L.Z. Gao, S. D. Huang*, “A rotor position correction method for high-speed permanent magnet synchronous motor based on current loop error correction”. Chinese Journal of Electrical Engineering, **vol. 37**, no. 8, Aug. 2017, pp. 2391-2398.
- [14] *C. Gu, X.L. Wang, & Z.Q. Deng*, “A dual phase-locked-loop based method for full compensation of rotor position estimation error in high-speed permanent magnet synchronous motors”. Chinese Journal of Electrical Engineering, **vol. 40**, no. 3, Mar. 2020, pp. 962-969.
- [15] *X. Q. Shi, X. L. Wang, T. X. Xu, & C. Gu*, “Self-searching optimal phase-shift correction strategy for high-speed brushless DC motors”. Journal of Electrotechnology, **vol. 34**, no. 19, Oct. 2019, pp. 3997-4005.
- [16] *C. Gu, X. Wang, F. Zhang, & Z. Deng*, “Correction of rotor position estimation error for high-speed permanent magnet synchronous motor sensorless drive system based on minimum-current-tracking method”. IEEE Transactions on Industrial Electronics, **vol. 67**, no. 10, Oct. 2020, pp. 8271-8280.